Periodica Polytechnica
Civil Engineering

61(3), pp. 361–380, 2017
https://doi.org/10.3311/PPci.9311

Comparative Approach to Seismic Vulnerability of an Elevated Steel Tank within a Reinforced Concrete Chimney

Yaniv Cohen[1,2], Arkady Livshits[2], Roberto Nascimbene[3,*]

RESEARCH ARTICLE

Received 07 April 2016; Revised 27 July 2016; Accepted 02 September 2016

Abstract

This study provides a framework for investigating the seismic response of an elevated steel water tank within a reinforced concrete chimney, to assist optimal tank placement and analyse different tank geometries. Elevated tank design procedures in different guidelines and codes are adequate for specific cases, none of which meets the exact requirements of this case study, in which the supporting structure mass is large relative to the storage tank. The tank is located at an elevation 63 m below the mid-height of the 200 m chimney, resulting in a different behavior than a simple cantilever. Furthermore, for certain H/R ratios, coupling effects may exist between the fundamental period of the chimney and that of the sloshing wave. An equivalent model is examined that is simple enough yet able to accurately produce the design acceleration, dynamic amplification, damping and torsional effects at the chosen tank location, and to capture site effects. An analysis of the tank at ground level is conducted according to AWWA D100-11. Then, the tank at elevation 63 m is analysed within the framework of three existing methods using code spectra and site-specific spectra. A novel fourth method is then proposed which, contrary to the existing methods, can accurately capture the conditions of this case study by combining the benefits of all methods. The workflow described here can be readily applied to other cases of elevated tanks for which the standard procedures are inadequate.

Keywords

steel tank, elevated tank, reinforced concrete chimney, non-structural component, dynamic amplification

[1]Istituto Universitario di Studi Superiori di Pavia
Università degli Studi di Pavia,
Piazza della Vittoria 15, 27100, Pavia
[2]Israel Electric Corporation ,
[3] European Centre for Training and Research in Earthquake Engineering,
EUCENTRE , via Ferrata 1, 27100 Pavia
*Corresponding author email: roberto.nascimbene@eucentre.it

1 Introduction

Elevated tanks are used in various processes in electrical power plants, all of which are designed giving high priority to safety considerations. As highlighted by Livaŏglu and Dŏgangün [1] and Hirde et al. [2], elevated storage tanks should remain functional in the post-earthquake period (Moslemi [3]), even after a major earthquake such the one that happened on 21st of July 1952 in California or the one in Chile on 22nd of May 1960 (Arze [4], Steinbrugge and Flores [5]), to ensure water supply for controlling fires, which cause a great deal of damage and loss of lives (Hirde et al. [2]). Nevertheless, several elevated tanks sustained moderate to severe damage during past earthquakes that happened in the past two decades: El Asnam, Algeria earthquake, 10/10/1980; Bihar-Nepal earthquake, 21/8/1988 (Jain and Sameer [6]); Jabalpur (Indian state of Madhya Pradesh) earthquake 22/5/1997 and Bhuj (state of Gujarat in India) earthquake, 26/1/2001 (Rai [7, 8, 9]); Maule earthquake, 27/2/2010 (Eidinger [10]); Van earthquake in Turkey, 23/10/2011 (Uckan et al. [11]).

Such performance reveals a complex behaviour mainly due to the presence of two primary components: the tank, which contains the liquid, and its supporting structure (this fact has been highlighted by Brunesi et al. [12] investigating the Emilia (Italy) earthquake, on 20/5/2012 and 29/5/2012). A wide variety in the configuration of elevated tanks can be found in civil engineering applications (Haroun and Ellaithy [13], Long and Garner [14]) and may be classified into three main categories as explicitly highlighted in FEMA 450 at Point 14.4.7.9:

1. frame elevated tanks with steel cross braced supporting towers (Shepherd [15]) or a reinforced concrete multi-column assembly (Bozorgmehrnia et al. [16]). Small-capacity (less than 0.76 ML) steel elevated tanks usually have a cylindrical sidewall, and an ellipsoidal bottom and roof; medium-capacity from 0.76 ML to 1.9 ML use torus bottom and ellipsoidal roofs, and large-capacity tanks (greater than 1.9 ML) may have a diameter from 11 to 20 m and a capacity from 750 to more than 3500 m^3;

2. axisymmetrical pedestal elevated tanks supported by a single circular steel or concrete tower (capacity less than 0.76 ML); or a single cylindrical support pedestal with a flared conical base (capacity from 0.76 ML to 7.6 ML) used to contain pumping units and other operating equipment;
3. composite elevated tanks comprised of a welded steel tank for watertight containment at the top and a single pedestal concrete support structure (Meier [17]). These tanks are also sometimes referred to as "concrete pedestal elevated tanks" (ACI 371R 98 and FEMA 450 Point 14.4.7.9.6) and use the best design features of both steel and concrete.

This study constitutes a fourth case to add to the above and deals with the case of a steel anchored water storage tank within a reinforced concrete chimney. It is located at an elevation of 63 m within the 200 m chimney, and serves as part of the Flue-Gas Desulfurization (FGD) system. It is designed to enable quick temperature lowering during a technical failure of the system, or during a sudden fire, earthquake or other natural disaster. The vertical location of the water tank (i.e. its relative elevation inside the chimney), must be verified considering the dynamic amplification and the ability of the tank to perform well in case of an earthquake, whilst also considering a variety of possible tank geometries.

With regards to dynamic amplification, two separate factors must be taken into account in the analysis: the first is the dynamic amplification of the tank components due to relative closeness to the natural periods of the systems, and the second is the dynamic amplification occurring along the chimney height.

In this study, different possible tank geometries are examined during an earthquake event, ranging from tanks with a low H/R ratio of 0.9, to tall slender tanks with an H/R ratio as high as 6.3 (H is defined herein as the water height, smaller than the total height of the tank wall, and R is the nominal radius). For all tank geometries considered, the properties, in addition to the maximum design overturning moment (M_f), and base shear of the tank, are calculated and compared by different design standards as the AWWA D100-11 [18] and the ASCE 7-10 [19].

In order to select the optimal geometry of the elevated tank and to confirm its location inside the chimney, while taking into consideration both the amplification of the acceleration along the chimney height and the possible dynamic amplification of the impulsive and convective components, the following steps have been followed:

Step I: The chimney, as the supporting structure of the tank, is examined according to the FEMA P-750 [20] document, followed by an elastic analysis of the chimney itself (construction of a combined model of the tank and chimney is a part of this step).

Step II: Eigenvalue analysis with different tank components (structure, impulsive, and convective). A simple two-mass model derived using basic dynamic equations is then used to better understand the phenomena. The examined parameters are defined and an analysis at ground level is performed based on AWWA D100-11 [18], using a simple spring-mass model, to determine the dynamic properties of the different tanks.

Step III: Evaluation of the forces using four different methods: Equivalent Static Analysis procedure for buildings supporting Non-Structural components (ESA-NS), Modal Response Spectra Analysis (RSA), RSA for Non-Structural components according to ASCE 7-10 Ch. 15 [19] referring to Ch. 13 (RSA-NS), and an extended procedure adapted specifically for this case study based on the RSA-NS (RSA-NS Extended).

Step IV: Comparison of the different methods used to estimate the forces in Step III using the code response spectra, and comparison of the site-specific and code response spectra.

2 STEP I: Analysis selection and Chimney/Tank model specifications

The site is located in Rutenberg, Ashkelon area, Israel. The region is considered a high seismic zone due to its closeness to the Dead Sea Transform which forms a boundary between the African and Arabian Plates. The hazard is defined according to the code spectra and site specific spectra. The acceleration response spectrum with the return period of 2475 years is presented in Fig. 1.

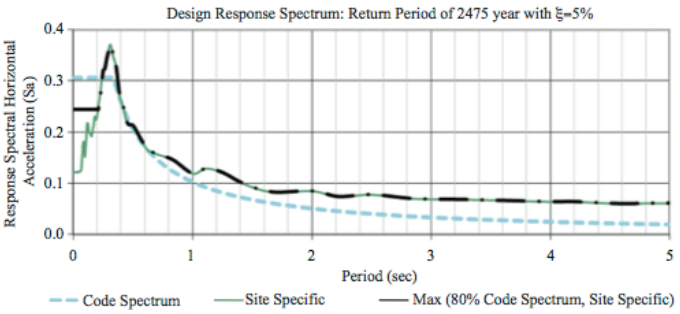

Fig. 1 Horizontal acceleration response spectrum with return period 2475 years and ξ=5%

It is important to select a clear and practical analysis procedure that complies with existing codes and regulations yet accounts for the specific features of the chimney and closely captures its predicted behaviour. Non-building structures require special analysis selection; when considering non-building structures similar to buildings, the procedure limitations are the same as for building structures, but non-building structures that are not similar to buildings exhibit a very different structural performance and behaviour. Non-building structures are subject to limitations in specific reference documents which address these differences, including publications by organizations such as ASCE, ASME, API, AWWA, and others. The ASCE 7-10 [19] is aligned with the NEHRP provisions [20] and refers to guidelines which are mostly empirical and provide details for adequate structural performance. The chimney is classified within the category of non-building structures not

similar to buildings. In this case, the FEMA P-750 [20] and ASCE 7-10 [19] documents refer to the ACI 307 [21] and the minimum requirements are always given by the FEMA P-750 provisions [20].

When selecting a method for performing dynamic analysis or determining the lateral force distribution for static analysis, several issues specified in ASCE 7-10 Ch.15 [19] must be addressed. Generally, a chimney with a relatively uniform mass distribution can be represented by a cantilever model, and then the equivalent lateral force procedure can be used. In our case study, however, several characteristics of the chimney which may affect its response preclude our ability to use this procedure, such as:

- openings in the chimney (Fig. 2) leading to stiffness/strength and torsional irregularities stemming from different resistance values in the horizontal and vertical directions, which increase its vulnerability. When following the ACI 307 [21] design procedure, chimneys may fail in a brittle and catastrophic manner around the openings (Wilson [22]). Non-uniform mass distribution along the chimney height also contributes to the irregularity. Particularly, Section 12.6 of NEHRP [20] details the analysis procedure based on the fundamental period T, and the presence of horizontal or vertical irregularities. When T is greater than or equal to $3.5T_s$ ($T_s = S_{D1}/S_{DS}$) the use of the equivalent lateral force procedure is not permitted; when this condition is satisfied, higher vibration modes contribute more significantly and cannot be neglected in comparison to the first mode contribution. Furthermore, tall reinforced concrete chimneys respond to earthquake excitation in a complex manner with the response being dominated by higher mode effects in the elastic (and inelastic) range (Wilson [22, 23]);

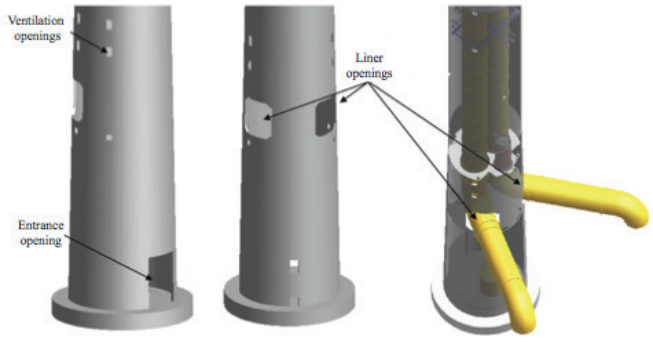

Fig. 2 Chimney openings leading to stiffness, strength and torsional irregularities

- in addition, the first period of the tank sloshing wave (convective component) and the first period of vibration of the chimney are close, especially for low H/R ratios, resulting in a coupling of the systems. Furthermore, higher mode periods of the chimney are close to those of the steel tank and the impulsive component (being rigidly attached to each other).

Clearly, a more precise analysis is required. The forces on the tank should not be extracted using the Equivalent Lateral Force on the chimney. Rather, the tank can be treated as a non-structural component since its weight is only ~2% of the combined weight. The ASCE 7-10 Ch.13 [19] then provides an Equivalent Static Analysis procedure for buildings supporting Non-Structural components (ESA-NS), which can be followed here since it does not account for the supporting structure. According to FEMA P-750 [20], judgement is required when deciding whether to treat a supported structure as a non-structural component or a non-building structure, and guidance on this process for seismic design is provided in Bachman and Dowty [24]. For instance, small tanks can be treated as non-structural components (provisions of Ch. 13 [19] and Table 13.6-1 [19]) while larger ones can be treated as non-building structures (provisions of Ch. 15 and/or Table 15.4-2 [19]). In fact, some of the non-structural components and non-building structures overlap (Gatscher and Bachman [25]).

As detailed above, ASCE 7-10 [19] is the appropriate code to refer to, when selecting the relevant analysis procedure. It provides minimum requirements and lists several categories into which the supporting and supported structures may fit, and gives design guidelines. If the supported structure weight is relatively small (W_{nb} < 25% of W_{tot}), then the effect on the overall nonlinear response is relatively small and the supported structure can be treated as a non-structural component (using Ch. 13 guidelines [19] - ESA-NS). The second case can occur if W_{nb} > 25% of W_{tot}, and the supporting structure is flexible, then the forces are determined considering effects of combined structural systems. In this case the combined design approach in code Section 15.3.2 [19] is used and dynamic analysis is performed (RSA-NS). Hence, the forces in this case study were evaluated using the following four methods:

- the Equivalent Static Analysis procedure for buildings supporting Non-Structural components (ESA-NS), in which the forces are estimated using ASCE 7-10 Ch.13 [19]. This method is somewhat oversimplified for our case study.
- the Modal Response Spectra Analysis (RSA), an extensively used procedure in force estimation. The chimney and tank are combined into a single model. The procedure is used in two ways: first, in a basic direct procedure without accounting for the limitations and second, in accordance with the ASCE 7-10 [19], the procedure serves as a basis for extracting the forces, accelerations, and amplifications.
- in order to perform the RSA, two methods are then used (RSA-NS; RSA-NS Extended). In the Response Spectra Analysis for Non-Structural components (RSA-NS), the design procedure is in accordance with ASCE 7-10

Ch.15 referring to Ch.13 [19]. As noted, this procedure refers to non-building structures supporting non-structural components. The chimney base shear and the actions from the analyses are used to derive the acceleration amplification along the height (a_i) and the tank dynamic amplification (a_p). In the Response Spectrum Analysis for Non-Structural components - Extended (RSA-NS Extended), a specific workflow for the purpose of this case study is designed and used, based on ASCE 7-10 Ch.15 and Ch.13 specifications [19].

A combined 3D model, using SeismoStruct [26], of the tank with flexible connections to the reinforced concrete chimney is used for Eigenvalue analysis and for RSA, RSA-NS, and RSA-NS Extended. The chimney is a strategic power plant facility. Thus, an accessible water storage facility must be readily available inside the chimney, to be used immediately in case of a sudden fire, earthquake or other natural disaster. The height of the chimney is 200 m, supported on a 3 m tall ring plate foundation connected with 48 concrete piles. The piles are 40 m long and 1.5 m in diameter. Thus, the chimney is modelled as a fixed-end connection pendulum (see also Livshits [28]). The chimney diameter narrows along the height, (base diameter of 23 m to top 20 m), with several large openings both at the base of the structure (8 m x 11 m) and at an elevation of 40 m (2 openings, 9 m x 9 m each; see Fig. 2). The wall thickness changes along the chimney height as detailed in Table 1.

Table 1 Chimney wall thickness distribution along the height.

Height [m]	Thickness[m]
0–75.5	0.70–0.35
75.5–150	0.35
150–200.5	0.70

These openings are modelled using a reduced moment of inertia, along with the original concrete cross-section area and mass distribution. A single reduced value was used in both directions, simplifying the analysis but neglecting torsional modes.

Two internal flue liners inside the chimney which are part of the flue gas desulphurization (FGD) process are modelled, in accordance with chimney liner standard, ASTM International Designation, D-5364-93 [27] (Fig. 3(a)). The chimney mass is distributed along the height (Fig 4 and Table 2), while the liners mass are lumped at the connection points, (Fig. 3(b,c)).

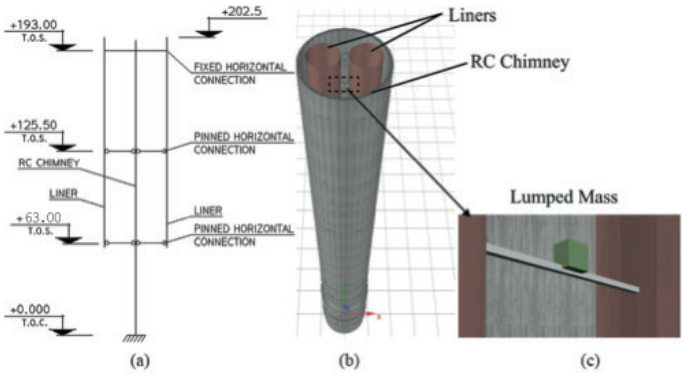

Fig. 3 (a) Vertical static scheme of the chimney and liner connections; Elevation 63 m, 125.5 m pinned horizontal connection only; (b) chimney model with liners inside; (c) elevation 193 m lumped mass and rigid connection to the chimney.

Most of the mass comes from the reinforced concrete, but several steel platforms (covered with concrete or grating) are distributed along the height for maintenance and mechanical equipment and are simply supported connections that do not add to the horizontal stiffness of the chimney. All the platforms at the different elevations are modelled by additional lumped masses at different elevations (Fig. 4).

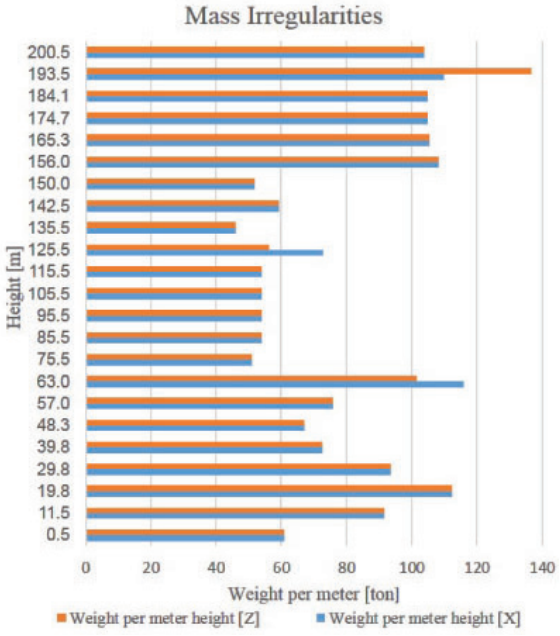

Fig. 4 Mass distribution along the height.

Table 2 Mass distribution values

Steel platform [ton]	Water tank [ton]	Liners [ton]	RC Chimney [ton]	Total mass [ton]
619	280	543	15114	16556

The tank is located at a 63 m elevation. A different model is used for each of the six cases of tank *H/R* ratios examined. The components are modelled by pendulums and concentrated masses. The masses and their heights are defined according to the tank dynamic properties at ground level using AWWA D100-11 [18]. The impulsive and steel structure components

(base, wall, and roof) are modelled with a stiff column while the convective mass is modelled with a flexible column. The *H/R* cases examined are combined into six models along with the chimney as the supporting structure. Two of these models from the AVEVA PDMS [29] software are presented in Fig. 5 along with the SeismoStruct [26] equivalent models.

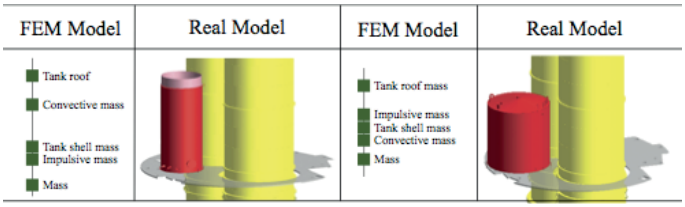

Fig. 5 Models of tank and chimney for two different H/R tank ratios from the AVEVA Plant Design Management System (PDMS) software [29] along with the equivalent models from SeismoStruct [26] in which the modelled tank components are represented as lumped masses placed at their center of mass.

3 STEP II: Eigenvalue analysis, examined parameters & dynamic properties

3.1 Eigenvalue analysis

The chimney, the convective component primary mode shapes, and the interaction between them are examined using basic dynamic principles. The tank and chimney can either be considered as two coupled SDOF systems or as a MDOF system, in which the natural periods of the combined system are determined using the equation of motion. The chimney first mode of vibration dominates with a period of 3.09 sec. When the separate SDOF system periods are close, i.e. 3-3.2 sec. for the tank, a coupling effect (or vibration resonance phenomenon) exists in the MDOF system and affects both the mode of vibration period and the dynamic amplification. A comparison of the SDOF system periods with those of the combined MDOF system as a function of the *H/R* ratio, accounting for the modal participation factor, is shown in Fig. 6. For SDOF-convective components with periods shorter than the SDOF-chimney period, the dominant period is elongated, which results in lower accelerations in the response spectra, while the opposite occurs for longer SDOF-convective component periods (e.g. tanks with low *H/R* ratios close to 1.0).

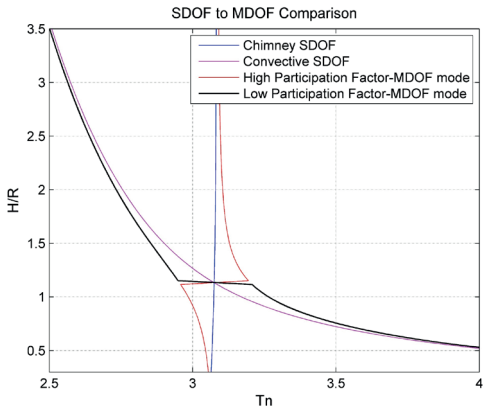

Fig. 6 Comparison of the period of SDOF separate system with combined 2-DOF system

Eigenvalue analysis is used to understand the chimney mode shapes which excite the tank and to examine each mass deflection according to the mode shape that excites it. Those mode shapes are then used in the RSA. A refined non-linear finite element model using fibre element (extensively verified through comparison with experimental results in case of steel structures (Grande and Rasulo [30], Wijesundara et al. [31]), reinforced concrete structures (Brunesi et al. [32, 33], Casotto et al. [34], Nascimbene [35]), masonry infill panels (Smyrou et al. [36]) and connections (Brunesi et al. [37]; Brunesi et al. [38])) allows the observation of the excitation of tank masses, as shown in Fig. 7 for the convective component, which has a flexible connection and thus undergoes a larger deflection compared to the impulsive component.

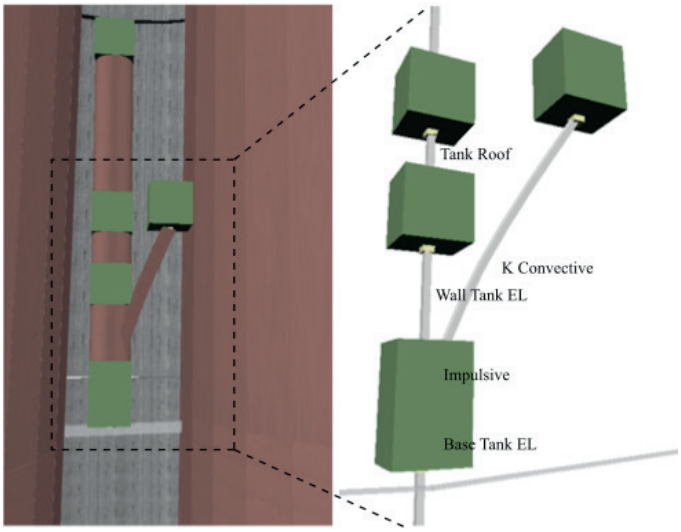

Fig. 7 Tank component lumped masses (base, wall, roof, impulsive, and convective components). The flexible connection of the convective component enables it to move much more than the others.

The fibre model results obtained using the MDOF 3D model were similar to those obtained with the basic dynamic equations. Elongation or shortening of the periods of different modes occurred as expected for different *H/R* ratios. In tall structures, higher modes affect longer periods than in short structures. This may result in closeness between the periods of the tank structure and its impulsive component and the period of the chimney higher modes. The effects are often more pronounced at higher elevations. In our case study, the convective component reduces the higher mode effects, so that for higher H/R ratios the modal participation factor of the higher modes is higher (for slender tanks ~20% while for squat tanks less than 15%).

3.2 Examined parameters and dynamic properties

Although this case study deals with an elevated tank rather than one placed at ground level, it was necessary to include a ground level analysis in order to compute the dynamic parameters of the different steel water tanks, such as impulsive mass, convective mass, and the relative elevation at which the equivalent

lateral force should be placed in order to calculate the overturning moments. The assumption, generally recognized in many standards on tanks worldwide from the European (Eurocode 8 Part 4 [39]) to the Indian one (IITK 2007 [40]), is that the ground level dynamic properties are similar to those at higher elevations. Following the Housner [41] model (Priestley et al., [42]), at ground level, the tank impulsive component is assumed to be rigidly attached to the tank structure (code equivalent model Fig. 8 (a)) and thus to have no effect on design acceleration which, for short periods, is defined at the plateau. The convective component period of vibration, defined by flexible springs, is usually dominated by the sloshing wave's first mode (the others contributing up to 6-7%, Priestley et al., [42]) and thus, following the US standard, the other modes are neglected and the equivalent simplified model presented in Fig. 8 (b) is used.

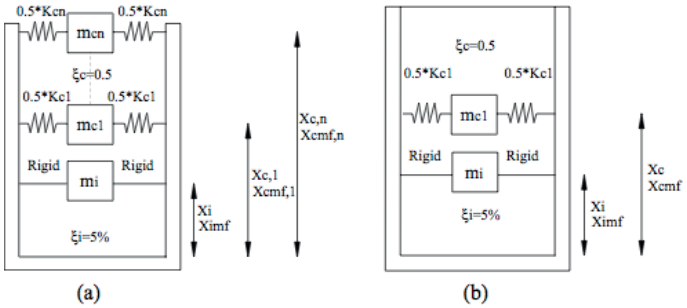

Fig. 8 (a) Mass-Spring model for code spectra; (b) simplified Mass-Spring model

In our case study or when using the site specific response spectra, the natural period of vibration of the structure and the impulsive component can both influence the results and are defined by a stiff spring (K_i, Fig. 9 (a) and (b)).

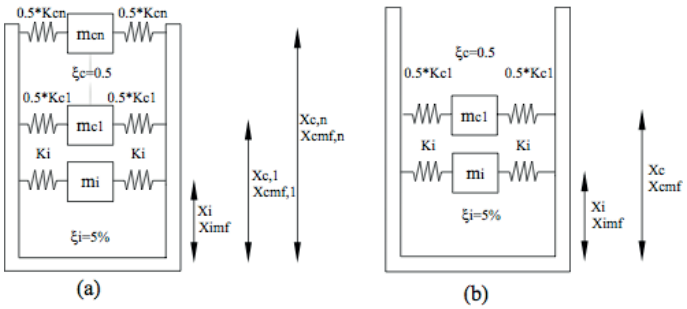

Fig. 9 (a) Mass-Spring model for site-specific spectra; (b) simplified Mass-Spring model for site-specific spectra.

The tank in the current study is large and thus treating it as a non-structural component results in an oversimplified model. Furthermore, the supporting structure had been located at the ground level, hence the tank would have been designed as a non-building structure according to the AWWA D100-11 [18] or the API 650 codes [43]. Instead of applying the force at the center of mass, a more precise approach is used here resembling the Housner [41] model, but adapting it as an equivalent simplified model for site-specific response spectrum as detailed in Fig. 9 (b). It is used throughout the analysis with the different methods to capture the dynamic amplification in both impulsive and convective components (with the exception of ESA-NS which only accounts for the supporting structure). This gives a closer approximation of the forces and moments in the tank. The design acceleration is defined using the acceleration response spectra (code spectra or site-specific). Depending on the method of choice, the acceleration is either defined as the maximum value (as for conservative methods), or derived from the equations as a function of the structure and component period, in which case dynamic properties can be accounted for at varying degrees of complexity (e.g., relative influence of the convective and impulsive components). The amplification along the height represents the design peak floor horizontal acceleration at the point of attachment of the tank, and depends on the attachment point. It can either be calculated directly, or estimated as a function of tank location. Accepted values range between 1.0 and 3.0, the lower bound representing an attachment at the structure base, and the higher bound representing attachment at the maximum structure height. The dynamic amplification factor depends on the way the tank is defined. When the tank is referred to as a non-structural component, according to Table 13.6-1 of ASCE 7-10 [19], the minimum requirement is a_p = 1.0. The tank is considered rigidly attached, and no distinction is made between the impulsive and convective components. The code, however, makes an exception; when component period > 0.06 sec it is considered a flexible non-structural component and the tank amplification used is a_p=2.5 (i.e. maximum possible amplification). When it is referred to as a non-building structure, the ability of capturing this phenomenon depends on the type of modelling. When the periods are close, the amplification reaches the maximum value, limited to 2.5 (limitation from the NCEER study in FEMA P-750 [20], defined as a function of T_p/T). For taller structures, and specifically for chimneys (Wilson [23]), the tank amplification may vary significantly due to higher mode effects. Thus, although code values range between 1.0-2.5, researchers have shown that much higher values can be obtained, 8 times the PGA (Fathali and Lizundia [47], see also Naeim [45]) and perhaps even higher for structures that are higher mode effect sensitive.

The torsional amplification factor (A_x), limited between 1.0 and 3.0, is defined in the ASCE 7-10 Eq.12.8-14 "Amplification of Accidental Torsional Moment" [19]. Various degrees of complexity are possible, but simplified models are often preferred over more complex ones, since understanding the dominant features to be considered in structural design is often satisfactory. Energy dissipation is a function of the following: free surface, wall-fluid interaction, and tank base-fluid interaction. AWWA D100-11 [18] and ASCE 7-10 [19] define 5% damping for the structure and the impulsive component. Most standards (including AWWA D100-11 [18] for ground level tanks) use

0.5% damping for the convective component to account for the friction of the tank wall and the liquid. According to the American code, there is a 1.5-factor difference in the actions when using 0.5% damping compared to 5% damping. In other guidelines (IITK-GSDMA Gujarat State Disaster Management Authority Guidelines for Seismic Design of liquid storage tanks [40]), the difference is as high as a factor of 1.75. The importance factor (I) for both components is defined as 1.5. When referring to the tank as a non-structural component, the same value is used and is addressed as I_p. As with building structures, the actions are reduced by dividing the forces by the force reduction factor, R. This factor represents the energy absorption capability of the tank and its attachments, which depend on both over-strength and deformability. Elevated tanks are typically provided with a greater safety margin, but use of ground level reduction factors is reasonable if the elevated tank and supporting structure are separate, as in our case. The impulsive and convective components reduction factors are defined separately, giving the former a lower value (since it depends only on the water energy dissipation), and the latter a higher value, since the steel tank structure and slab connections can dissipate more energy.

Table 3 Design reduction factor for different codes

		ASCE 7-10 [19]		AWWA D100-11 [18]		API 650 [43]	
		R_i	R_c	R_i	R_c	R_i	R_c
Steel tank (above ground)	Anchored	3.0	1.5	3.0	1.5	4.0	2.0
	Unanchored	2.5	1.5	2.5	1.5	3.5	2.0

		ASCE 7-10 [10]		AWWA D100-11 [18]	
		R_i	R_c	R_i	R_c
Elavated tanks	Shaft type	2.0a	1.5	3.0c	1.5c
	Frame type	3.0b	1.5	3.0d	1.5

		ACI 350.3 [46]		ACI 371.3R [47]	
		R_i	R_c	R_i	R_c
Elavated tanks	Shaft type	2.0	1.0	2.0	-
	Frame type	-	-	-	-

a) Used also in cases of unbraced legs or asymmetrically braced legs for a frame type tank

b) Symmetrically braced legs

c) Used for steel pedestal type tanks

d) Tanks with tension only diagonal bracing in column-braced and column-supported elevated tanks

The tank here is anchored to the rigid concrete slab. Anchored tanks generally have greater reserve of strength to resist seismic overload compared to unanchored ones designed using annular plate detailing. Proper anchoring design provides a shell attachment and an embedment detail that can yield the bolt without pulling it from the foundation or tearing the shell. Thus, in our case a larger reduction factor is taken to allow a greater safety margin. For elevated tanks, different values are given for shaft-type vs. frame type supporting structures. A comparison between the values in three USA documents (ASCE 7 [19], AWWA D100 [18], and API 650 [43]) is provided in Table 3. Least conservative are the values suggested by API 650 [43]. The ACI 350.3 [46] and ACI 371.R [47] (not used herein) provide even more conservative values.

Note that when referring to the tank as a non-structural component, the reduction factor is addressed as R_p. According to ASCE 7-10 Ch.13 Table 13.6-1 [19] this value is equal to 2.5.

3.3 Calculation of the Dynamic Properties according to the Ground Level Procedure (AWWA D100-11)

The ground level design procedure detailed in AWWA D100-11 [18] is followed, taking into account the tank impulsive and convective components, solely to calculate the parameters for the other methods. The relative masses and heights are determined. Six tank cases at ground level, differing in their H/R ratios, are examined. The water volume is constant, and the actions are divided into 3 components: inertia force (tank structure: base, wall, and roof with additional live load which takes into account storage area); impulsive component; and convective component. The dynamic properties of the tanks, calculated according to AWWA D100-11 [18], are presented in Tables 4.

Table 4 AWWA D100-11 [18] Ground Level Dynamic Properties for Tanks (cont.).

Units: Ton, kN, m	Case A	Case B	Case C
H/R	6.4	4.0	2.0
Volume [m^3]	262	262	262
H [m]	15	11	7
D [m]	4.7	5.5	6.9
R [m]	2.4	2.8	3.5
T_c [sec]	2.27	2.45	2.75
T_i [sec]	0.16	0.13	0.07
Mass empty tank [ton]	17	16	16
Mass convective/ Mass tot	7%	12%	23%
Mass Convective [ton]	19	30	59
K convective [kN/m^2]	145	198	310
X_c [m]	13.72	9.50	5.21
X_i [m]	7.06	4.98	2.85
X_{cmf} [m]	13.72	9.50	5.29
X_{imf} [m]	7.78	5.83	3.91

Table 4 AWWA D100-11 [18] Ground Level Dynamic Properties for Tanks (cont.).

Units: Ton, kN, m	Case D	Case E	Case F
H/R	1.2	1.0	0.9
Volume [m^3]	262	262	262
H [m]	5	4.5	4
D [m]	8.2	8.6	9.1
R [m]	4.1	4.3	4.6
T_c [sec]	3.02	3.13	3.29
T_i [sec]	0.06	0.05	0.05
Mass empty tank [ton]	17	17	18
Mass convective/ Mass tot	37%	42%	48%
Mass Convective [ton]	96	110	127
K convective [kN/m^2]	416	444	463
X_c [m]	3.20	2.75	2.34
X_i [m]	1.88	1.69	1.50
X_{cmf} [m]	3.65	3.41	3.32
X_{imf} [m]	3.36	3.45	3.61

4 STEP III: Force evaluation with code spectra using different methods

The methods used are as follows: ESA-NS (article 4.1), RSA (article 4.2), RSA-NS (article 4.3), and RSA-NS Extended (article 4.4).

4.1 Equivalent Static Analysis for Non-Structural Components (ESA-NS)

The ESA-NS method is based on the procedure in ASCE 7-10 Ch.13.3 [19] for non-structural components, generally used for short to moderate height structures. For taller structures, higher mode effects can bring about a variation in the amplification with the structure height (see also Miranda and Taghavi [48]). Furthermore, the horizontal ESA-NS design force equation may be inaccurate for longer-period and irregular structures. Nevertheless, this method was considered here due to the weight criterion introduced in the code, which states that the tank should be treated as a non-structural component, being only ~2% of the combined weight. The horizontal forces are calculated using the following expression:

$$F_{ph} = \frac{0.4 S_{DS} a_p}{\frac{R_p}{I_p}} (1 + 2\frac{z}{h}) \mathrm{W}_p \qquad (1)$$

where W_p is the tank weight, and PGA=0.4S_{DS} is the amplification of the Peak Ground Acceleration along the structure height, derived from the ASCE7-10 spectrum [19], by dividing the maximum possible acceleration at the site (S_{DS}) by 2.5.

The term 0.4 S_{DS} (1 + 2 (z/h)) in Equation 1 represents the design peak floor horizontal acceleration at the non-structural component attachment point; z is the attachment height relative to the base. This expression accounts for the increase in shaking intensity on the supporting structure upper levels, and is independent of the non-structural system. ESA-NS accounts only for the supporting structure and thus, the tank simplified equivalent model is not accounted for. The ASCE 7-10 [19] amplification uses a simple linear profile along the building height which captures only the first mode response resulting in a maximum value of 3 times the PGA at the top of the building. The coefficients I_p, R_p, are defined as in ASCE 7-10 Ch.13 (Table 5) [19]. As detailed above, the average period of both components is much higher than 0.06 sec, and thus, following the comment in Table 5, a_p=2.5 is used.

Table 5 ASCE 7-10 Ch.13 [19] except from table 13.6-1 Seismic: Coefficients for Mechanical and Electrical Components.

	Importance Factor (I_p)	Reduction Factor (R_p)	Dynamic Amplification (a_p)
Steel tank	1.5	2.5	1.0*

*If the component period is more than 0.06 sec, the dynamic amplification is ap=2.5

The tank damping is defined by the supporting structure response spectrum. The code defines lower and upper bounds on the horizontal design force; this prevents the product of the individual factors from producing an unreasonably high force, considering the expected nonlinear response of the supports and components. As the maximum forces were derived for nonlinear behaviour and our case is more elastic, the reduction of forces will be different. Contrary to the horizontal forces, the vertical seismic forces are considered without dynamic amplification, in accordance with the code. For computing the moments, the vertical and horizontal forces obtained above are applied at the center of mass of the non-structural component. The results for ESA-NS are presented in Tables 6. In this method, all the components are considered equally dynamically amplified and the PGA's amplification does not depend on the supporting structure. The ESA-NS does not take into account the tank geometry; rather, the shear is relatively high and constant for all different tanks examined. The resisting moment is calculated using the tank self-weight minus the vertical seismic component. As expected, the only situation in which overturning may pose a problem is for very slender tanks. The ESA-NS M_f overturning moment and base shear are shown in Fig. 10 in comparison with the ground level results.

Table 6 Actions: Equivalent Static Analysis for Non-Structural Components (ESA-NS) FEMA P-750 [20] and ASCE 7-10 [19]. Code response spectrum return period 2475 years (cont.).

Parameters	Case A	Case B	Case C
Height Amplification (1+2*z/H)	1.63	1.63	1.63
Component Dynamic Amplification (a_p)	2.5	2.5	2.5
Importance factor (I_p)	1.5	1.5	1.5
Reduction factor (R_p)	2.5	2.5	2.5
Minimum F_{ph} [kN]	353	353	353
Maximum F_{bh} [kN]	1881	1881	1881
F_{ph} [kN]	819	819	819
% of seismic weight	30%	30%	30%
F_{pv} [kN]	167	167	167
$H/2$ [m] center of mass	7.5	5.5	3.5
M_{otm} ESA-NS [KN]	6120	4488	2856
Resisting vertical moment and self weight	13.72	9.50	5.21

Table 6 Actions: Equivalent Static Analysis for Non-Structural Components (ESA-NS) FEMA P-750 [20] and ASCE 7-10 [19]. Code response spectrum return period 2475 years (cont.).

Parameters	Case D	Case E	Case F
Height Amplification (1+2*z/H)	1.63	1.63	1.63
Component Dynamic Amplification (a_p)	2.5	2.5	2.5
Importance factor (I_p)	1.5	1.5	1.5
Reduction factor (R_p)	2.5	2.5	2.5
Minimum F_{ph} [kN]	353	353	353
Maximum F_{bh} [kN]	1881	1881	1881
F_{ph} [kN]	819	819	819
% of seismic weight	30%	30%	30%
F_{pv} [kN]	167	167	167
$H/2$ [m] center of mass	2.5	2.25	2
M_{otm} ESA-NS [KN]	2040	1836	1632
Resisting vertical moment and self weight	9815	10346	10973

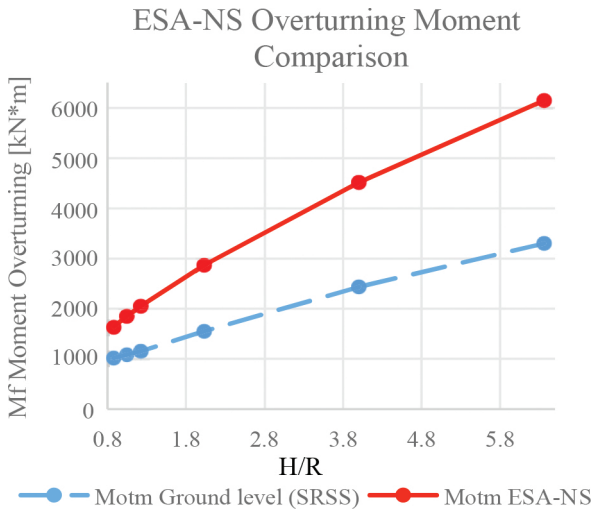

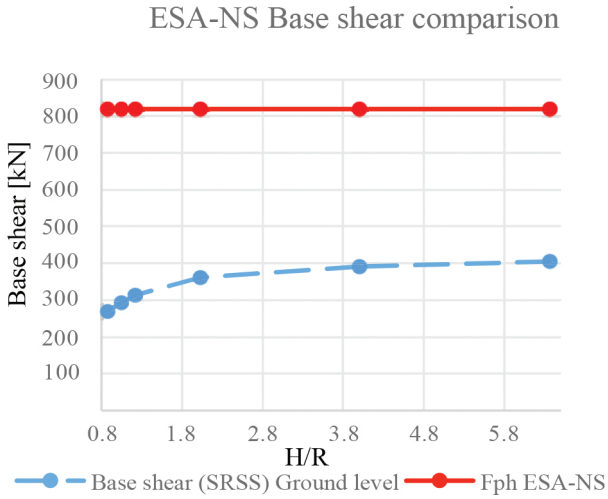

Fig. 10 ESA-NS: overturning moment and tank base shear in comparison to ground level results

4.2 Modal Response Spectrum Analysis (RSA) using combined model

The actions on the tank at elevation 63 m are evaluated using the combined chimney and the tank 3D SeismoStruct [26] model by modal RSA with 5% damping. The flexibility of the impulsive and convective components is accounted for in the model through the stiffness of the attaching element using the simplified equivalent model for the site specific case. An elastic analysis is performed; therefore, the spectrum can be linearly multiplied by coefficients later in the analysis to extract the actions. The importance factor used here is I=1.5 as in all other methods. The ground level seismic coefficients according to the AWWA D100-11 code [18] (presented in Table 3, R_i=3.0, R_c=1.5) are used for the tank components. For the convective component, the response spectrum with 0.5% damping is needed and is accounted for by using a factor of 1.5 for the actions. The responses for each of the modes are then combined using the SRSS rule. The results for the modal RSA method are presented in Table 7. Amplification occurs in the convective component when the periods of the first mode of the chimney and the first mode of the sloshing wave are close. The RSA Mf overturning moment and base shear are shown in Fig. 11.

Table 7 Actions response Spectrum Analysis (RSA), code response spectrum, return period of 2475 years.

Units: kN, m	Case A	Case B	Case C
M_f Overturning (SRSS)	2035	1468	932
M_f structure	185	147	114
M_f impulsive	1846	1316	810
M_f convective	129	124	124
Base shear (SRSS)	262	253	241
V_f structure	25	27	33
V_f impulsive	237	226	207
V_f convective	9	13	23
% of seismic weight	10%	10%	9%

Units: kN, m	Case D	Case E	Case F
M_f Overturning (SRSS)	895	1139	707
M_f structure	100	102	94
M_f impulsive	533	490	446
M_f convective	632	974	457
Base shear (SRSS)	264	341	219
V_f structure	40	45	47
V_f impulsive	159	142	124
V_f convective	173	285	138
% of seismic weight	10%	13%	9%

Fig. 11 RSA: overturning moment and tank base shear

4.3 Modal Response Spectrum Analysis for Non-Structural Components with ASCE 7-10 Requirements

Modal RSA-NS (RSA-NS; FEMA P-750 Ch.15.3.1 [20] referring to ASCE 7-10 Eq.13.3-4 [19]) is used to improve accuracy and to account for the flexibility and coupling between the periods of the tank components and the chimney. When following the code procedure, as with ESA-NS, some limitations on amplification exist. Eq. (2) is used to calculate the horizontal force:

$$F_{ph} = \frac{a_i \, a_p}{\frac{R_p}{I_p}} A_x \, W_p \tag{2}$$

where W_p is the component weight. The equivalent simplified model for site specific is used as detailed above for RSA. The procedure for non-structural components defines one mass; it is divided into different components to capture the different dynamic amplifications. After extracting the horizontal forces these are summed and applied at the center of mass as defined in the code. The acceleration a_i and the factor a_p are extracted in accordance with FEMA P-750 guidelines [20]. The elastic values from the modal response spectrum reflect the combined model dynamic characteristics. The design amplification and acceleration vary with the component period and location along the chimney height, and are determined using the actions derived here.

A modal analysis is performed without considering the chimney ductility (see justifications for elastic behaviour of the chimney FEMA E-74 [49]). As noted, the ASCE 7-10 guidelines [19] call for use of elastic values and thus, a reduction factor of R=1.0 is taken for the chimney. The base shear is then calculated, and compared to that obtained using the equivalent lateral force procedure. According to the code requirements, the modal analysis base shear should not be less than 85% of the equivalent lateral force base shear. The acceleration (a_i) is computed from the modal RSA analysis actions. The total shear just below elevation 63 m is divided by the seismic weight at and above 63 m. A comparison of the RSA-NS method results to those obtained using ESA-NS in accordance with ASCE 7-10 code requirements [19], is presented in Fig. 12. The results for the RSA-NS are a function of the chimney stiffness and mass distribution and thus, are unique to this specific chimney. The different tank geometries exhibit a similar shape of amplification along the height. ESA-NS is conservative, especially at elevation 63 m where there is no amplification of the acceleration (Table 8). From elevation 140 m the amplification values increase rapidly up to the chimney top, where the PFA reaches 2.5 times the PGA (Fig. 12). The results for this method are similar to those obtained by Fathali and Lizundia [44]; in that work, the authors compared data from buildings with the ASCE 7-10 equations [19] used to design acceleration sensitive non-structural components. They found that for long period buildings (with a period of over 1.5 sec), the amplification for the relationship between z/h and PFA/PGA is considered very conservative.

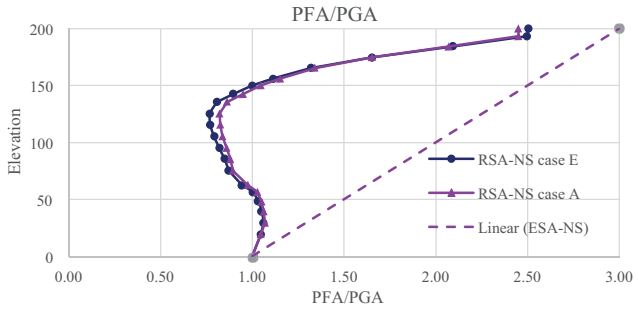

Fig. 12 Amplification of the peak floor acceleration (PFA) with respect to the peak ground acceleration (PGA)

To extract the component amplification factor (a_p), the shear force at the point of component attachment is taken from the modal analysis and divided by the component weight. This results in the product $a_i a_p$ which is the peak floor acceleration with the component dynamic amplification. Finally, $a_i a_p$ is divided by a_i which was determined in the previous step and the resulting value is used in Eq. 13.3-4 from ASCE 7-10 [19]. This enables separate procedure application to each tank component, resulting in different a_p values. Although the dynamic amplification for case E reaches values greater than 5.0, the value applied in the design is 2.5 in accordance with code limitations (maximum value of a_p=2.5 and minimum value of a_p=1.0). The analysis results are presented in Fig. 13 and Table 8, and agree with the basic dynamic equation results (Step II). For case E, the resulting acceleration is lower than for the other cases, due to a tuned mass damping effect.

Table 8 Component acceleration and dynamic amplification

	case A	case B	case C	case D	case E	case F
a_i for El 63 [g]	0.052	0.052	0.052	0.051	0.049	0.051
Impulsive $a_p=a_i^* a_p/a_i$	2.50	2.50	2.50	2.50	2.50	2.50
Convective $a_p=a_i^* a_p/a_i$	1.00	1.00	1.00	2.50	2.50	2.17

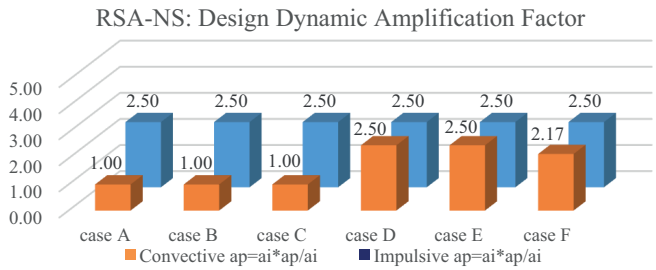

Fig. 13 Non-structural component dynamic amplification factor determined using RSA-NS with ASCE 7-10 limitations

The reduction and importance factors (R_p, I_p) are defined according to ASCE 7-10 Ch.13 Table 13.6-1 (same as for the ESA-NS method) [19]. The torsional amplification factor is defined in accordance with code section "Amplification of Accidental Torsional Moment" A_x=1.0, as detailed above. The RSA-NS method is the only procedure (except for RSA-NS Extended) that accounts for additional torsional factor effects that are not captured in the analysis or the model. The damping is defined as 5%, according to the supporting structure. The results for the RSA-NS method are presented in Table 9. The RSA-NS M_f overturning moment is shown in Fig. 14. As evident below, this method does not capture the dynamic amplification for low *H/R* ratios. Therefore, a reduction in the actions occurs rather than the opposite.

Table 9 Actions: Responce Analysis for Non-Structural Components (RSA-NS), code response spectrum, return period of 2475 years (SeismoStruct [26])

Units: kN, m	Case A	Case B	Case C
M_f Overturning (SRSS)	1562	1108	673
M_f structure	149	118	91
M_f impulsive	1412	989	579
M_f convective	44	51	64
Base shear (SRSS)	208	201	192
V_f structure	20	21	26
V_f impulsive	188	180	165
V_f convective	6	9	18
% of seismic weight	8%	7%	7%
Units: kN, m	**Case D**	**Case E**	**Case F**
M_f Overturning (SRSS)	430	364	312
M_f structure	79	77	73
M_f impulsive	311	240	192
M_f convective	182	180	165
Base shear (SRSS)	172	162	156
V_f structure	32	34	37
V_f impulsive	124	107	96
V_f convective	73	80	83
% of seismic weight	6%	6%	6%

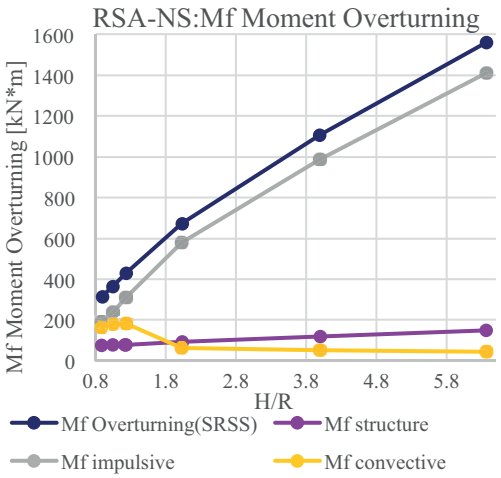

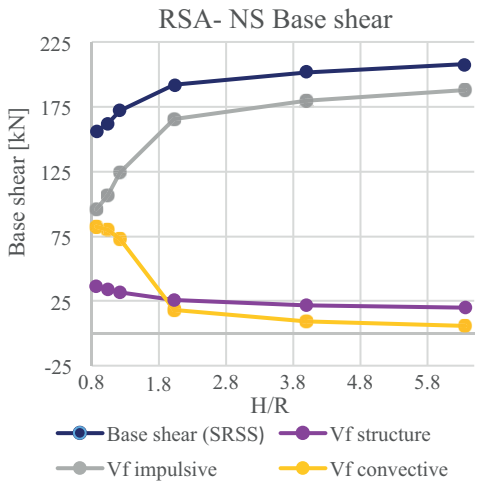

Fig. 14 RSA-NS: overturning moment and tank base shear

4.4 Proposed Design Procedure for the Case Study: Modal RSA Non-Structural Extended (RSA-NS Extended)

Our proposed design procedure RSA-NS Extended is based on the tank dynamic properties from the ground level AWWA D100-11 [18] procedure, in combination with ASCE 7-10 Ch.15.3.1 [19] which refers to Eq. 13.3-4 in ASCE 7-10 Ch. 13. The design forces for the tank structure, impulsive component (Eq. (3)) and convective component (Eq. (4)) are computed in accordance with Eq. 13.3-4 of ASCE 7-10 (see also Eq. (2) and accompanying text):

$$F_{ph,imp.} = \frac{a_i a_{p,imp.}}{\frac{R_{imp.}}{I_p}} A_x W_{imp.} \tag{3}$$

$$F_{ph,conv.} = \frac{a_i a_{p,conv.}}{\frac{R_{conv.}}{I_p}} A_x W_{conv.} \tag{4}$$

As noted, the workflow of the standard does not fully capture the requirements of our specific case study and thus, several adaptations have been made in our proposed design method. Of course, it is imperative to assure that the minimum requirements recommended by the standard are met, but all the while an extended and more elaborate procedure can provide a better estimate of the design forces. This is critical because the structure in our case study is part of an essential facility, and the designer should take into account the necessity to perform well under failure and provide better safety measures. Both the AWWA D100-11 [18] elevated tank procedure and the ASCE 7-10 Ch.13 [19] for non-structural components neglect the sloshing effect in the tank. The convective contribution cannot be ignored, especially for tanks with a low *H/R* ratio for which the sloshing effect is influential. For both the impulsive and convective components, an equivalent spring model can capture the components' dynamic amplification by RSA. The acceleration and dynamic amplification are extracted as with RSA-NS. The equivalent simplified model for site specific spectra is used and instead of applying the force at the center of mass and following the code procedure for non-structural components, a more precise approach is used resembling the Housner [41] model. In addition, the reduction factors according to the AWWA D100-11 [18] are used defining it as a non-building structure. To extract the floor acceleration (a_i), and the component dynamic amplification factor (a_p), the procedure detailed above regarding RSA-NS is followed according to ASCE 7-10 Eq.13.3-4 [19], with the exception that here (RSA-NS Extended), the actual maximum amplification from the analysis is considered (larger than 2.5) along with a minimum requirement from the code of a_p=1.0, as shown in Table 9.

Table 9 Component acceleration and dynamic amplification

Units: kN, m	Case A	Case B	Case C
a_i El 63 [g]	0.052	0.052	0.052
Impulsive $a_p=a_i*a_p/a_i$	3.78	3.77	3.75
Convective $a_p=a_i*a_p/a_i$	1.00	1.00	1.00
Units: kN, m	**Case D**	**Case E**	**Case F**
a_i El 63 [g]	0.051	0.049	0.051
Impulsive $a_p=a_i*a_p/a_i$	3.83	3.99	3.87
Convective $a_p=a_i*a_p/a_i$	3.57	5.33	2.17

The dynamic amplification factors used here are shown (for the different tank cases) in Fig. 15. Clearly, both the impulsive and convective components are affected by system coupling; this is especially evident for tanks with a low *H/R* ratio, where the impulsive component is heavily influenced by the higher mode effects, and the convective component is influenced by the first mode of vibration.

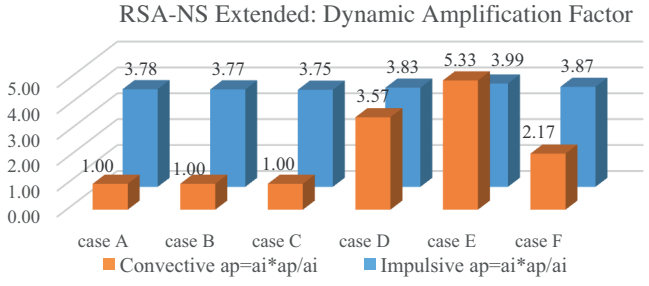

Fig. 15 RSA-NS Extended: Dynamic amplification factor used to calculate the actions

The damping is defined according to the AWWA D100-11 [18] (for elevated tanks) and the ASCE 7-10 standards [19] as the default value of 5%. The AWWA D100-11 [18] for elevated tanks considers only the impulsive component and disregards the convective component, and the ASCE 7-10 [19] non-structural component procedures (e.g. ESA-NS) use 5% damping according to the supporting structure. Especially for tanks with

low H/R ratios, where the contribution of the convective component is large, 5% damping might not be conservative. Neither the AWWA D100-11[18] nor the ASCE 7-10 [19] distinguishes between the different materials of which the tank structure is composed. For concrete structures, the damping ratio is usually 5% and for steel structures 2% damping is usually applied, and values can be even lower if the connections in the structure are mostly welded rather than bolted. The value used here is in accordance with the IITK-GSDMA guidelines [40], which recommend using 2% damping for the impulsive component in steel storage tanks. Linear interpolation of the values is not possible since acceleration values vary logarithmically with the damping (Newmark and Hall [50]); however, because an elastic analysis is performed, it is possible to linearly multiply the actions by a factor of 1.2 (according to the nonlinear Equation (5) taken from the EC8 [39]) to account for the amplification brought about by using 2% damping instead of 5%:

$$EC8\ \ part1:\eta=\sqrt{\frac{10}{5+\xi}}>0.55 \qquad (5)$$

The convective component 0.5% damping is accounted for by using a 1.5 factor according to the American code. The analysis results for the RSA-NS Extended method are presented in Table 11.

Table 11 Component acceleration and dynamic amplification

Units: kN, m	Case A	Case B	Case C
M_f Overturning (SRSS)	2436	1759	1121
M_f structure	224	177	137
M_f impulsive	2206	1573	968
M_f convective	160	176	193
Base shear (SRSS)	314	303	289
V_f structure	30	32	39
V_f impulsive	283	270	247
V_f convective	12	19	36
% of seismic weight	12%	12%	11%
Units: kN, m	**Case D**	**Case E**	**Case F**
M_f Overturning (SRSS)	1070	1362	846
M_f structure	120	122	113
M_f impulsive	637	586	533
M_f convective	756	1164	546
Base shear (SRSS)	316	408	262
V_f structure	48	54	56
V_f impulsive	190	170	148
V_f convective	207	341	165
% of seismic weight	12%	16%	10%

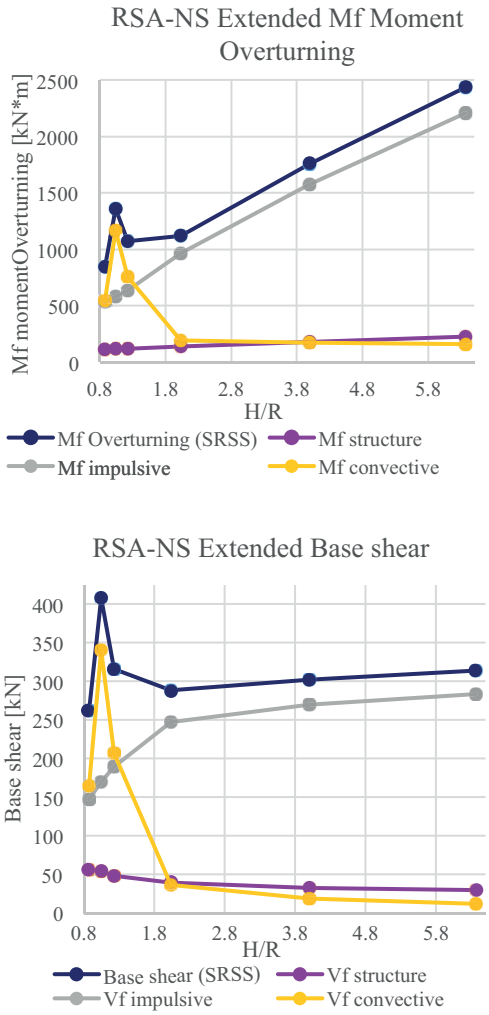

Fig. 16 RSA-NS Extended: overturning moment and tank base shear

The RSA-NS Extended M_f overturning moment and base shear are shown in Fig. 16. As evident for the low *H/R* ratios, this method captures dynamic amplifications for coupled systems for both the convective and impulsive components. Table 12 provides a summary of the different analysis methods, highlighting differences in the parameters used in each method.

Table 12 Parameters comparison

Parameter	ESA-NS	RSA	RSA-NS	RSA-NS Extended
Equivalent Simplified Model	Not accounted	Model dependent	Model and code dependent	Model and code dependent
Design acceleration (a)	a=PGA=0.4S_{DS}	a=Sa(T_n supporting structure from the analysis)	a=Sa(T_n supporting structure from the analysis)	a=Sa(T_n supporting structure from the analysis)
Amplification along the structure height	Linear: 1+2(z/h) values:1.0-3.0	a_i*a_p/a_i "black box"	Developed from the analysis results using a_i*a_p/a_i	Developed from the analysis results using a_i*a_p/a_i
Component dynamic amplification factor (a_p)	ASCE 7-10 [19] Non-structural components Table 13.6-1: a_p=1.0* *for flexible component a_p=2.5	Analysis dependent	Analysis dependent, Min: a_p=1.0 Max: a_p=2.5	Analysis dependent, Min: a_p=1.0 Max: No limit
Torsional amplification factor (A_x)	Not accounted	Model dependent	Model and code dependent	Model and code dependent
Damping (ξ)	Supporting structure dependent	Supporting structure dependent	Fixed 5% Impulsive, 0.5% Convective	Material components dependent
Importance Factor (I)	Engineering judgement I_p=1.0-1.5	Engineering judgement I=1.0-1.5	Engineering judgement I_p=1.0-1.5	Engineering judgement I=1.0-1.5
Reduction Factor (R)	ASCE 7-10 [19] Non-structural components Table 13.6-1: R_p=2.5	AWWA D100-11 [18]: Table 28 Anchored at ground level Parameters: $R_{impulsive}$=3.0 $R_{convective}$=1.5	ASCE 7-10 [19] Non-structural components Table 13.6-1: R_p=2.5	AWWA D100-11 [18]: Table 28 Anchored at ground level Parameters: $R_{impulsive}$=3.0 $R_{convective}$=1.5

5 STEP IV: Comparison of the different methods

Decision-making and optimization of structure characteristics, while complying with code regulations, are crucial in the design process, especially in this study, in view of the facility importance and performance requirements even under an extreme event. Attempting to use a "default" design procedure may produce very different results. In this section, the methods used in our case study are compared based on the following central design factors: floor acceleration, component dynamic amplification factor, higher mode effects, damping, reduction factor, equivalent model, action comparison and site specific and code response spectra.

5.1 Equivalent model

For ESA-NS and RSA-NS, the horizontal force is applied at the center of mass. RSA and RSA-NS Extended follow the AWWA D100-11 standard [18], in which the horizontal force is applied at the equivalent center of pressure that may develop on the tank wall during an event. For calculating the moment, the standard distinguishes between the bottom base wall moment and the overturning moment, and provides a different level arm for the impulsive and convective components (X_{imf}, X_i, X_{cmf}, X_c, respectively). Similar to the AWWA D100-11 elevated tank procedure [18], ESA-NS and RSA-NS apply the total (equivalent) force that may develop at the center of mass without accounting for the impulsive and convective components. Also, in ESA-NS, the convective component is neglected and the moment is defined as the overturning moment. The level arm for moment calculation, based on equations from the AWWA D100-11 standard [18], is presented in Fig. 17. As shown below, for extremely slender or squat tanks the force can be applied at the center of mass; otherwise it is conservative.

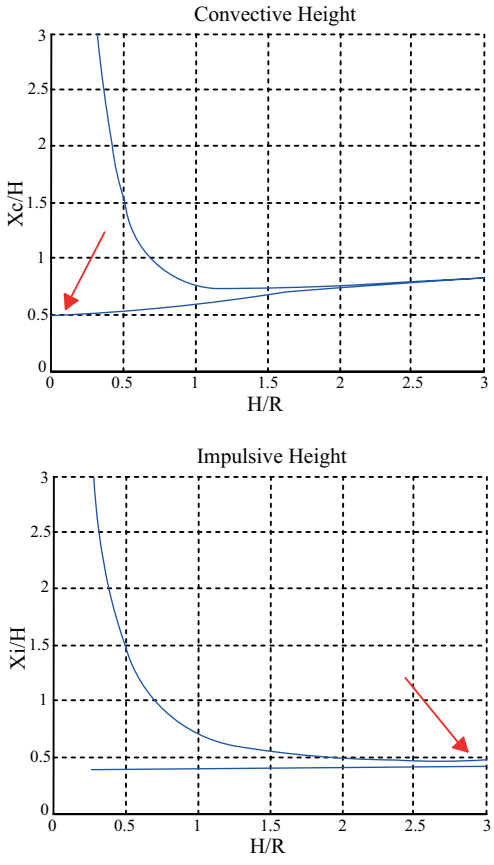

Fig. 17 Convective and impulsive height for the force location according to the AWWA D100-11 [18]

As shown in Fig. 18, it is more conservative to consider the equivalent horizontal force at the center of mass rather than at the location of the pressure. This is shown for RSA-NS Extended, but applies also to all other methods.

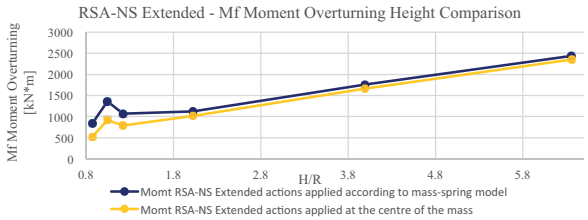

Fig. 18 Code Spectra, RSA-NS Extended Overturning moment, comparison of the height coordinate for the equivalent horizontal force

5.2 Floor Acceleration

The RSA, RSA-NS, and RSA-NS Extended methods all account for the design acceleration at the tank location through the modal analysis. In RSA, the acceleration at the connection point is a function of the different modes, while in RSA-NS and RSA-NS Extended, its value is derived from the base shear. Thus, when using software to extract the forces with RSA, the acceleration value is sometimes lost in the results. Modal RSA accounts for the different *H/R* ratios, as shown in Fig. 19. The acceleration for case E is lower than for the other cases and brings about a TMD effect on the chimney; however in this specific case, the effect is negligible. ESA-NS is excessively conservative, and does not account for the differences in *H/R* ratios. As evident in Fig. 19, in both cases, A and E, despite the large difference in geometry, the accelerations for calculation of the design forces are the same. The acceleration is independent of the supporting structure properties, and the supporting structure period is ignored. Furthermore, the peak ground acceleration (PGA) is amplified linearly according to a general first mode that may be adequate only for low to mid-height buildings. In addition, it has been shown that higher modes affect the acceleration more than the displacement and should be considered in the amplification profile. Therefore, the accelerations are always larger than the PGA; for tall structures with a long period, in which the accelerations are generally lower, this may result in unnecessarily large actions. The peak floor acceleration used for elevation 63 m in the different methods is presented in Fig. 19.

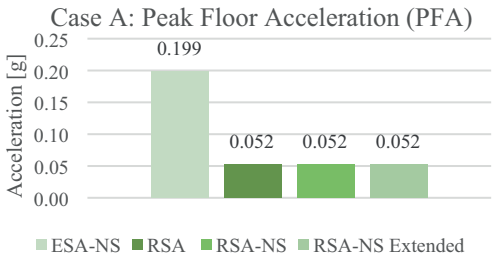

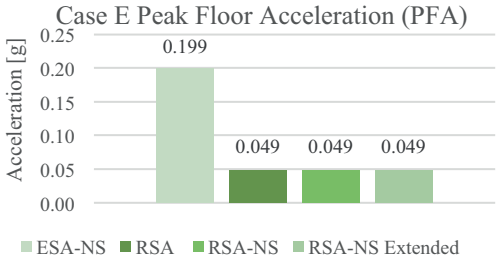

Fig. 19 Case A vs. Case E: Comparison of the PGA according to the different methods

5.3 Component Dynamic Amplification Factor

For ESA-NS and RSA-NS, the ASCE 7-10 guidelines [19] specify upper and lower bounds for a_p. The upper bound limitation is applied here although, as noted earlier, studies have shown that, especially for coupled systems, the amplification can greatly exceed 2.5. As noted, ESA-NS does not account for the tank *H/R* ratio or the period of the supporting structure; this is even more pronounced when the periods of the supporting structure and the convective component are close and a much larger amplification may occur (as in case E; see Fig. 20). In ESA-NS, the amplification is limited to two values: 1.0 for a rigid component or 2.5 for a flexible one. The tank is thus defined rigid here, although its period is longer than 0.06 sec which enables defining it as flexible. The RSA and RSA-NS Extended do not specify an upper bound for the amplification. Both have the same high amplification values, capturing higher mode effects and coupled systems (see Fig. 20). RSA-NS Extended, however, sets a minimum bound for the ground level amplification (1.0; in case D the factor obtained from RSA was 0.77). The advantage of RSA-NS Extended is that it accounts for the minimum amplification as in the code, and the designer is able to understand the magnitude of the factor used in the analysis. In RSA, the amplification is lost in the results and in some cases (slender tanks) it does not meet the minimum code requirements. The tank dynamic amplification used for elevation 63 m according to the different methods is presented in Fig. 20.

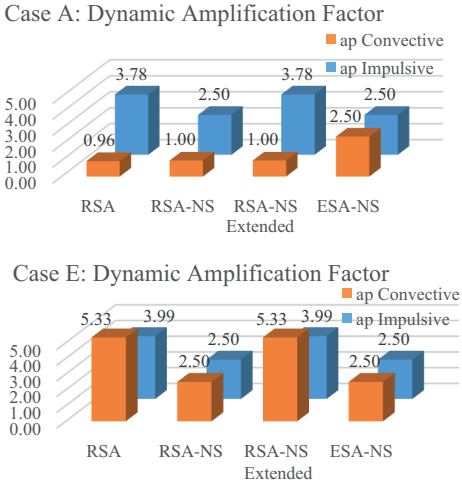

Fig. 20 Case A vs Case E: Dynamic amplification factor for different methods

5.4 Higher Mode Effects

RSA, RSA-NS and RSA-NS Extended all account for higher mode effects through the dynamic amplification factor. This influences the tank structure and impulsive components which are both attached to the chimney by a stiff-spring connection that is sensitive to these modes. The convective component is modelled by a flexible connection and is influenced by the supporting structure's first mode. The upper region of the chimney is more sensitive to higher mode effects than low and mid-level heights. ESA-NS is defined and used for low to mid-height buildings where higher mode effects are not as influential. Therefore, the equation does not account for these modes.

5.5 Damping

Analyses for all the methods are performed with a response spectrum of 5% damping. RSA and RSA-NS follow the ASCE 7-10 [19] which refers to AWWA D100-11 [18] and defines 5% damping for the impulsive and tank structure component, regardless of the material. ESA-NS defines damping according to the supporting structure rather than by tank structure or content. For the case of a slender concrete tank, 5% damping would have been a close approximation of the actual damping. According to the literature, for a squat steel tank, 2% damping should be applied to account for steel connections. The convective component for which 0.5% damping is applied here (in all methods except ESA-NS) has a substantial role for low *H/R*

5.6 Reduction Factor

The reduction factor for RSA-NS and ESA-NS is defined according to ASCE 7-10 Ch.13 [19], where each non-structural component is assigned a different factor. The tank is assigned a single value of 2.5 for both the impulsive and convective components, which simplifies the design but renders it somewhat less accurate for tanks that are either extremely slender or extremely squat. Both RSA and RSA-NS Extended apply the reduction factor according to the AWWA D100-11 ground level procedure [18], where a separate factor is specified for each component, improving method accuracy.

5.7 Shear & Moment

As exemplified in Figures 21, 22 and 23, large differences exist in the shears and moments obtained using each method. ESA-NS is too conservative, whereas RSA-NS is non-conservative. RSA-NS Extended captures the higher demand for shear in the low *H/R* ratio tanks. It accounts for material-specific damping characteristics, and for the amplification due to very close periods of the supporting system and tank components, and results in larger actions than the code requirements. In this case study, a high amplification occurs for the low *H/R* ratio (case E). RSA and RSA-NS Extended capture this phenomenon. For these methods, the actions are larger for low *H/R* ratio tanks than for slender tanks (case A). The actions obtained using RSA-NS, however, are reduced instead. A comprehensive comparison of the actions is shown in Fig. 21 to 23. As noted, ESA-NS shear is conservative and does not rely on tank *H/R* ratios. Furthermore, as expected, slender tanks (e.g. case A) have a higher overturning moment.

5.8 Site specific and code response spectra

The results obtained for the site specific response spectra are quite similar to those obtained using code spectra, with some exceptions related to a higher dynamic amplification; in this case study, a certain range of frequencies is amplified by the inherent site characteristics. Generally, methods that capture the dynamic amplification show that low *H/R* ratio tanks, with a longer sloshing wave period, are more affected. ESA-NS results are the same for both types of response spectra.

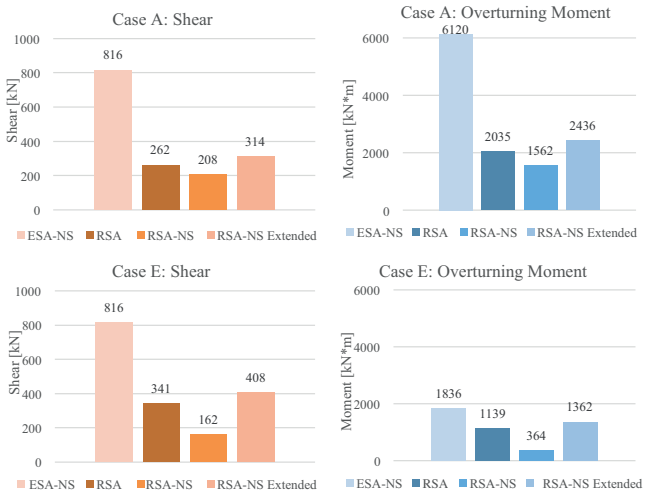

Fig. 21 Code Spectra, Case A and Case E shear and overturning moment comparison

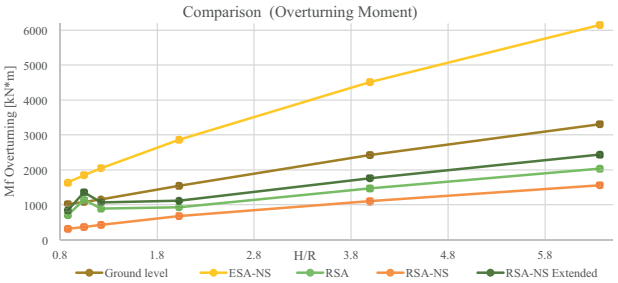

Fig. 22 Code Spectra, overturning moment comparison

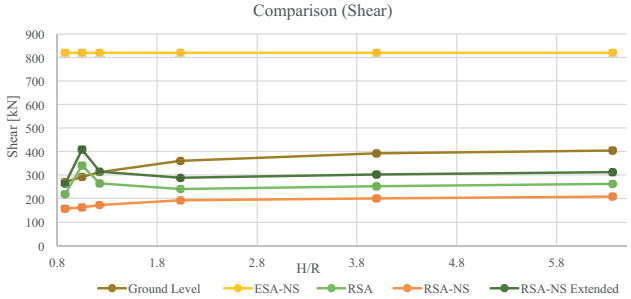

Fig. 23 Code Spectra, base shear comparison

As shown above, when the convective component period matches the chimney fundamental period, this may result in a tuned mass damper (TMD) that affects the period of the structure, and therefore also the design acceleration. Different frequency ranges are amplified differently in the code and site-specific spectra. Thus, the chimney base shear obtained using modal RSA results in different reductions of the actions for each spectrum. A comparison of the TMD effect when using code and site-specific spectra is shown in Table 13. For the code spectra, when comparing case A to case E (where the tank is a TMD) the base shear is reduced by 3%, while for the site-specific spectra there is a 9% reduction.

Table 13 Chimney Base Shear (TDM effect)

Units: kN	Case A	Case B	Case C
Code spectra	8808	8800	8791
Site-specific spectra	9907	9901	9903
Units: kN	**Case D**	**Case E**	**Case F**
Code spectra	8703	8539	8666
Site-specific spectra	9694	9080	9630

The resulting actions are compared in Fig. 24 and 25. Due to a coupling between the periods of the tank convective component and the fundamental period of the chimney (case E) for the site-specific spectra, the overturning moment is not conservative and was underestimated (Fig. 24; RSA and RSA-NS Extended). While RSA and RSA-NS Extended captured the amplification due to the coupling, RSA-NS not only did not capture the amplification, but showed a reduction in the shear and the overturning moment.

Thus, when selecting the proper analysis method, designers should be aware of potential sources of coupling between the structures. For slender tanks, all methods (with the exception of ESA-NS) provide more or less similar results and can in principle be used interchangeably

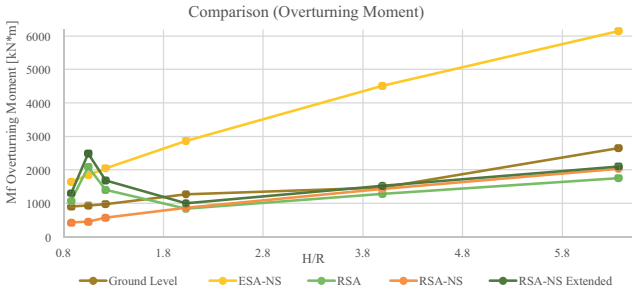

Fig. 24 Site-specific, overturning moment comparison

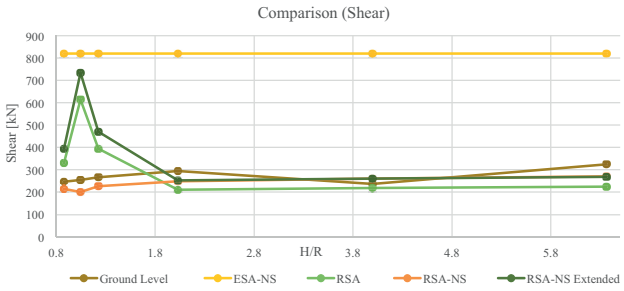

Fig. 25 Site-specific, base shear comparison

6 Summary and conclusions

The codes provide detailed and specific procedures for the case of elevated tanks in which the dominant portion of the total mass is located at the top of the supporting structure, resulting in a cantilever first mode. When the supporting structure period is coupled with the tank component, an amplification related to resonance phenomena occurs. In this case, the use of the code procedure for elevated tanks is not permitted, and alternative methods are used to calculate the actions that may develop during an earthquake. None of these methods, however, fully captures the actual actions that may develop for a wide range of tank *H/R* ratios. The key findings of this work will be briefly summarized below:

1. The proposed method, RSA-NS Extended, follows the RSA-NS procedure but captures the actual dynamic amplification, and applies a lower bound to it in order to avoid the possibility of attenuation. ESA-NS is overly conservative (especially for slender tanks, with the exception of case E) and inadequate for the case of an RC chimney as the supporting structure. The RSA method is a "black box" that accounts for amplifications. Analysis of the actions, however, reveals that in some cases, attenuation occurs rather than amplification, providing results for the component dynamic amplification that are lower than ground level (and the minimal code requirement of a_p=1.0). RSA-NS provides the necessary information related to the acceleration and the amplification. However, due to several issues – the reduction factor used, the equivalent force location, and the code limitations on the amplification, the resulting actions are very low, rendering it inaccurate for use here. For instance, with the geometry of case E in our study, for which the convective component period is close to that of the chimney, an amplification of the actions (as with the other methods) was expected but rather, these limitations resulted in the opposite.
2. Site characteristics substantially affect both the supporting structure and the tank. The spectral accelerations for periods shorter than 0.2 sec are lower than the code spectra. For periods in the range of 0.2-0.4 sec, a large local amplification occurs, and in general for long periods there is a higher spectral acceleration than the

code spectra. In ESA-NS, the maximum code spectral acceleration values are used. The other methods (RSA, RSA-NS, RSA-NS Extended) account for the different modes; the convective component is influenced by long period values which are higher for the site-specific spectra, and the impulsive and tank structure components are influenced by short period spectra values which are lower for the site-specific spectra.

3. When coupling occurs, the dynamic amplification of the tank components may reach values much higher than the code. In the site-specific spectra, the convective component reaches an amplification value greater than 8, and in the code spectra the value is larger than 5. Even the impulsive and tank structure components, which were analysed with stiff-spring connections, are dynamically amplified by a factor of 4 due to higher mode effects. These results are in agreement with several studies (e.g. Naeim [45], Fathali and Lizundia [44]), which claim that the upper bound limitation of a_p=2.5 may be too low. As evident from the results of this case study, this is especially true for the case of tall reinforced concrete chimneys.
4. The model proposed for the RSA-NS Extended, resembling the Housner [41] mechanical model of the equivalent spring–mass system, should be used with the reduction factors defined in the AWWA D100-11 ground level procedure [18].
5. When the convective component period matches the fundamental period of the chimney, this may result in a TMD that reduces the design acceleration for the chimney, but amplifies the actions on the tank. Earthquakes are usually dominated by a wide range of frequencies, and thus, using the tank as a TMD is not an optimal solution, since this type of TMD operates in a narrow band of frequencies. For the code spectra, when comparing case A to case E (where the tank is a TMD) the base shear is reduced by 3% and for the site-specific spectra by 9%.
6. Torsional effects, which may be important in the design and detailing of the structure, are sometimes reduced or neglected altogether. A reduction of the torsional effects in this case study is a result of the common approach of applying the spectra in one direction and using a simplified model (the effect of the openings in the chimney are not fully captured here albeit the work by Livshits [28] and Wilson [2] that has indicated that it can be influential).
7. Comparison of the obtained results suggests that the preferred method of choice, which provides the most accurate results for the actions for all different tank geometries (*H/R* ratios) and both for the code and site-specific spectra, is the RSA-NS Extended. This is most evident in cases where coupling occurs, and in other cases in which the values obtained using this method exceed even those obtained using conservative methods.

Acknowledgement

We are grateful to M. Cademartori, S. Pucciano, and D. Cicola for fruitful discussions, and to Laurie Cohen for reading and editing the manuscript.

We also wish to thank I.E.C. for encouraging research on Earthquake Engineering.

References

[1] Livaŏglu, R., Dŏgangün, A. "Simplified seismic analysis procedures for elevated tanks considering fluid-structure-soil interaction." *Journal of Fluids and Structures*. 22 (3), pp. 421-439. 2006. DOI: 10.1016/j.jfluidstructs.2005.12.004

[2] Hirde, S., Bajare, A., Hedaoo, M. "Seismic performance of elevated water tanks." *International Journal of Advanced Engineering Research and Studies*. I (1), pp. 78-87. 2011.

[3] Moslemi, M. "Seismic response of ground cylindrical and elevated conical reinforced concrete tanks." Ph.D Thesis, Ryerson University, Toronto, Ontario, Canada. 2011. http://digital.library.ryerson.ca/islandora/object/RULA:1666

[4] Arze, E. "Seismic failure and repair of an elevated water tank." In: Proceedings of the 4th World Conference on Earthquake Engineering, Santiago, Chile, Vol. III, pp. B6-57-B6-69. 1969. http://www.iitk.ac.in/nicee/wcee/article/4_vol3_B6-57.pdf

[5] Steinbrugge, K. V., Flores, R. A. "The Chilean earthquakes of May, 1960: a structural engineering viewpoint." *Bulletin of the Seismological Society of America*. 53 (2), pp. 225-307. 1963. http://www.bssaonline.org/content/53/2/225.abstract

[6] Jain, S. K., Sameer, S. U. "A review of requirements in Indian codes for aseismic design of elevated water tanks." *Bridge & Structural Engineering IABSE*. 23 (1), pp. 1-16. 1993. http://www.iitk.ac.in/nicee/skj/Research_Papers/AseismicDesignofElevatedWaterTanks.pdf

[7] Rai, D. C. "Seismic retrofitting of R/C shaft support of elevated tanks." *Earthquake Spectra*. 18 (4), pp. 745-760. 2002. DOI: 10.1193/1.1516753

[8] Rai, D. C. "Review of code design forces for shaft supports of elevated water tanks." In: Proceedings of the 12th Symposium on Earthquake Engineering, IIT Roorkee, India, Dec. 16-18, 2002. pp. 1407-1418. 2002. http://citeseerx.ist.psu.edu/viewdoc/download?doi=10.1.1.525.6941&rep=rep1&type=pdf

[9] Rai, D. C. "Performance of elevated tanks in Mw 7.7 Bhuj earthquake of January 26th, 2001." *Proceedings of the Indian Academy of Sciences - Earth and Planetary Sciences*. 112 (3), pp. 421-429. 2003. http://home.iitk.ac.in/~dcrai/details/BhujEQ.pdf

[10] Eidinger, J. M. "Performance of water systems during the Maule Mw 8.8 earthquake of 27 February 2010." *Earthquake Spectra*. 28 (S1), pp. S605-S620, 2012. DOI: 10.1193/1.4000038

[11] Uckan, E., Akbas, B., Shen, J., Wen, R., Turandar, K., Erdik, M. "Seismic performance of elevated steel silos during Van earthquake, October 23, 2011." *Natural Hazards*. 75 (1), pp. 265-287. 2015. DOI: 10.1007/s11069-014-1319-9

[12] Brunesi, E., Nascimbene, R., Pagani, M., Beilic, D. "Seismic performance of storage steel tanks during the May 2012 Emilia, Italy, Earthquakes". *Journal of Performance of Constructed Facilities*. 29 (5), 04014137. 2015. DOI: 10.1061/(ASCE)CF.1943-5509.0000628

[13] Haroun, M. A., Ellaithy, H. M. "Seismically induced fluid forces on elevated tanks." *Journal of Technical Topics in Civil Engineering*. 111 (1), 1-15. 1985. http://cedb.asce.org/CEDBsearch/record.jsp?dockey=0046834

[14] Long, B., Garner, B. "*Guide to storage tanks & equipment*." 588 p. Professional Engineering Publishing. 2004. http://www.wiley.com/WileyCDA/WileyTitle/productCd-1860584314.html

[15] Shepherd, R. "The seismic response of elevated water tanks supported on cross braced towers." In: Proceedings of the 5th World Conference on Earthquake Engineering, Rome, Italy, Session 2B, Vol. I. pp. 640-649. 1974. http://www.iitk.ac.in/nicee/wcee/article/5_vol1_640.pdf

[16] Bozorgmehrnia, S., Ranjbar, M. M., Madandoust, R. "Seismic behavior assessment of concrete elevated water tanks." *Journal of Rehabilitation in Civil Engineering*. 1 (2), pp. 69-79. 2013. http://civiljournal.semnan.ac.ir/article_8_1.html

[17] Meier, S. W. "Today's composite elevated storage tanks." In: 2002 AWWA Conference & Exposition, New Orleans, LA. 2001. http://tankindustry.com/websites/tankindustry/images/technicalpapers/todays_composite_elevated_storage_tanks.pdf

[18] American Water Works Association (AWWA). "Welded steel tanks for water storage." AWWA D100, Colorado, USA. 2011.

[19] ASCE. "Minimum Design Loads for Buildings and Other Structures." ASCE 7, American Society of Civil Engineers, Virginia, USA. 2010. http://ascelibrary.org/doi/book/10.1061/asce7

[20] Federal Emergency Management Agency (FEMA). "NEHRP Recommended Seismic Provisions for New Buildings and Other Structures." FEMA P-750, Washington D.C., USA. 2009. https://www.wbdg.org/ccb/DHS/fempp750.pdf

[21] American Concrete Institute. "Code Requirements for Reinforced Concrete Chimneys (ACI 307-08) and Commentary." ACI 307, 2008. https://www.concrete.org/store/productdetail.aspx?ItemID=30708

[22] Wilson, J. L. "Earthquake response of tall reinforced concrete chimneys." *Engineering Structures*, 25 (1), pp. 11-24. 2003. DOI: 10.1016/S0141-0296(02)00098-6

[23] Wilson, J. L. "Code recommendations for the seismic design of tall reinforced concrete chimneys." CICIND Report, Vol. 6, No. 2. 2000. http://www.iitk.ac.in/nicee/wcee/article/0051.pdf

[24] Bachman, R. E., Dowty, S. M. "Is it a Nonstructural Component or a Nonbuilding Structure?" *Structure Magazine*. pp. 18-21. July, 2008. http://www.structuremag.org/wp-content/uploads/2014/08/C-CS-NonstructuralComp-Bachman_Dowty-July081.pdf

[25] Gatscher, J. A, Bachman, R. E. "Elements of 2012 IBC / ASCE 7-10 Non-structural Seismic Provisions: Bridging the Implementation Gap." In: 15 WCEE, Lisbon, Portugal. 2012. http://www.iitk.ac.in/nicee/wcee/article/WCEE2012_2385.pdf

[26] Seismosoft. "SeismoStruct v7.0 – A computer program for static and dynamic nonlinear analysis of framed structures." 2014.

[27] ASTM International. "Standard guide for design, fabrication, and erection of fiberglass reinforced plastic chimney liners with coal-fired units." ASTM D5364, 2002. https://www.astm.org/Standards/D5364.htm

[28] Livshits, A. "Concrete chimney analysis and design: FE models and ANSYS-based CAD." In: 8th International ANSYS Conference, Pittsburgh, USA. 1998.

[29] AVEVA, PDMS. "PDMSV 12.1.sp2 - Plant Design Management System." 3D CAD design software, 2014.

[30] Grande, E., Rasulo, A. "Seismic assessment of concentric X-braced steel frames." *Engineering Structures*. 49, pp. 983-995. 2013. DOI: 10.1016/j.engstruct.2013.01.002

[31] Wijesundara, K. K., Nascimbene, R., Rassati, G. A. "Modeling of different bracing configuration in multi-storey concentrically braced frames using a fiber-beam based approach." *Journal of Constructional Steel Research*. 101, pp. 426-436. 2014. DOI: 10.1016/j.jcsr.2014.06.009

[32] Brunesi, E., Nascimbene, R. "Extreme response of reinforced concrete buildings through fiber force-based finite element analysis." *Engineering Structures*. 69, pp. 206-215. 2014. DOI: 10.1016/j.engstruct.2014.03.020

[33] Brunesi, E., Nascimbene, R., Parisi, F., Augenti, N. "Progressive collapse fragility of reinforced concrete framed structures through incremental dynamic analysis." *Engineering Structures*. 104, pp. 65-79. 2015. DOI: 10.1016/j.engstruct.2015.09.024

[34] Casotto, C., Silva, V., Crowley, H., Nascimbene, R., Pinho, R. "Seismic fragility of Italian RC precast industrial structures." *Engineering Structures*. 94, pp. 122-136. 2015. DOI: 1 0.1016/j.engstruct.2015.02.034

[35] Nascimbene, R. "Numerical model of a reinforced concrete building: earthquake analysis and experimental validation." *Periodica Polytechnica Civil Engineering*. 59 (4), pp. 521-530. 2015. DOI: 10.3311/PPci.8247

[36] Smyrou, E., Blandon, C., Antoniou, S., Pinho, R., Crisafulli, F. "Implementation and verification of a masonry panel model for nonlinear dynamic analysis of infilled RC frames." *Bulletin of Earthquake Engineering*. 9 (5), pp. 1519-1534. 2011. DOI: 10.1007/s10518-011-9262-6

[37] Brunesi, E., Nascimbene, R., Rassati, G. A. "Response of partially-restrained bolted beam-to-column connections under cyclic loads." *Journal of Constructional Steel Research*. 97, pp. 24-38. 2014. DOI: 10.1016/j.jcsr.2014.01.014

[38] Brunesi, E., Nascimbene, R., Rassati, G. A. "Seismic response of MRFs with partially-restrained bolted beam-to-column connections through FE analyses." *Journal of Constructional Steel Research*. 107, pp. 37-49. 2015. DOI: 10.1016/j.jcsr.2014.12.022

[39] The European Union Per Regulation. "Eurocode 8: Design of structures for earthquake resistance – Part 4: Silos, tanks and pipelines." EN 1998-4. 2006. https://law.resource.org/pub/eu/eurocode/en.1998.4.2006.pdf

[40] Indian Institute of Technology Kanpur - Gujarat State Disaster Management Authority. "IITK-GSDMA Guidelines for Seismic Design of Liquid Storage Tanks." 2007. http://www.iitk.ac.in/nicee/IITK-GSDMA/EQ08.pdf

[41] Housner, G. W. "The dynamic behaviour of water tanks." *Bulletin of the Seismological Society of America*. 53 (2), pp. 381-387. 1963.

[42] NZSEE. "Seismic design of storage tanks." Recommendations of a study group of the New Zealand National Society for Earthquake Engineering. 2009. http://www.nzsee.org.nz/publications/storage-tanks/

[43] American Petroleum Institute (API). "Welded storage tanks for oil storage." API 650, Washington D.C., USA. 2007. https://law.resource.org/pub/us/cfr/ibr/002/api.650.2007.pdf

[44] Fathali, S., Lizundia, B. "Evaluation of the ASCE/SEI 7 Equations for Seismic Design of Nonstructural Components using CSMIP Records." In: Proceeding of SMIP12 Seminar on Utilization of Strong-Motion Data, Sacramento, California. pp. 1-18. 2012. http://www.conservation.ca.gov/cgs/smip/docs/seminar/SMIP12/Pages/P1_Paper_Fathali_Lizundia.aspx

[45] Naeim, F. "Performance of Extensively Instrumented Buildings during the January 17, 1994 Northridge Earthquake - An Interactive Information System." Report No. 7530-68, John A. Martin Associates, Inc., Los Angeles, USA. 1997. https://caltech.tind.io/record/670988

[46] American Concrete Institute. "Seismic Design of Liquid-Containing Concrete Structures and Commentary." ACI 350.3, Farmington Hills, MI., USA. 2006.

[47] American Concrete Institute. "Guide for the analysis, design, and construction of concrete-pedestal water towers." ACI 371R, Farmington Hills, MI., USA. 1998. https://www.concrete.org/store/productdetail.aspx?ItemID=37198&Format=DOWNLOAD

[48] Taghavi, S., Miranda, E. "Response assessment of non-structural building elements." 84 p. Pacific Earthquake Engineering Research (PEER) Center, Berkeley, California, USA. 2003. https://searchworks.stanford.edu/view/5579251

[49] Federal Emergency Management Agency (FEMA). "FEMA E-74 Reducing the Risks of Non-structural Earthquake Damage." Washington D.C., USA. 2012. https://www.fema.gov/fema-e-74-reducing-risks-nonstructural-earthquake-damage

[50] Newmark, N. M., Hall, W. J. "*Earthquake spectra and design*." 103 p. Earthquake Engineering Research Institute, Berkeley, USA. 1982. https://www.amazon.com/Earthquake-Engineering-monographs-earthquake-structural/dp/0943198224